RSC Pharmaceutics

Accepted Manuscript

This article can be cited before page numbers have been issued, to do this please use: M. A. Tomeh, G. Hoover, S. Horst, E. De Leeuw, M. Chengalvala, R. J. Shattock and A. Watkinson, *RSC Pharm.*, 2026, DOI: 10.1039/D6PM00134C.

View Article Online
DOI: 10.1039/D6PM00134C

Marburg self-amplifying mRNA-lipid nanoparticle vaccine: differential effects when co-formulated with Toll-like Receptor Agonists.

Mhd Anas Tomeh[1], Gillian Hoover[2], Sarah Horst[2], Erik de Leeuw[2], Murty Chengalvala[2], Robin Shattock[3] & Allan Watkinson[1]

[1]BioCMC, Labcorp, York, UK; [2]Antibody Reagents & Vaccines, Labcorp, Denver, PA, USA; [3]Department of Infectious Disease, Imperial College, London, UK.

Abstract

The emergence of Marburg disease in parts of Africa poses a global threat with the potential to spread to other regions. This requires rapid development of effective vaccines to be used as countermeasures in case of an outbreak of Marburg virus. This study evaluates the impact of Toll-like Receptor (TLR) agonists on the adaptive immune response to a self-amplifying mRNA (saRNA) vaccine targeting the Marburg virus glycoprotein (GP), delivered via lipid nanoparticles (LNPs). The base saRNA-LNP formulation demonstrated high encapsulation efficiency, stability, and immunogenicity in mice, confirming its potential as a vaccine candidate. To investigate the changes in immune responses, three Toll-like Receptor (TLR) agonists—MPLA (TLR4), CpG ODN (TLR9), and Telratolimod (TLR7)—were co-formulated with the saRNA-LNPs. Each agonist required tailored formulation strategies due to distinct physicochemical properties, achieving >90% encapsulation efficiency and maintaining critical quality attributes. CryoEM revealed structural variations, including blebbing in CpG and Telratolimod formulations. *In vivo* studies showed that MPLA significantly enhanced B-cell responses, while Telratolimod and CpG had minimal impact on IgG levels. T-cell analysis revealed that Telratolimod and MPLA suppressed IFN-γ responses. Overall, these findings demonstrate that co-formulation with TLR agonists resulted in differential immune responses, where MPLA augmented humoral responses, the TLR9 agonist CpG provided no benefit and the TLR7 agonist Telratolimod inhibited responses, particularly with respect to cellular immunity.

Introduction

Marburg virus (MARV) is a highly infectious zoonotic pathogen on the WHO pandemic watchlist that causes a severe, rapidly spreading hemorrhagic fever with mortality rates up to 88%[1 2]. Because of its significant global health risk and the current lack of an approved countermeasure, developing a licensed vaccine remains a major unmet medical need[3 4].Several research teams are working on developing an MVD vaccine, with modalities ranging from inactivated virus, virus-like particles (VLPs), subunit vaccines, DNA vaccines and adenovirus vector vaccines. MVD

View Article Online
DOI: 10.1039/D6PM00134C

vaccine research has generally focused on leveraging knowledge gained from studies on related Ebola virus, given their structural and pathogenic similarities[5]. More specifically, the antigenic target for many of the MVD development vaccines has been the MARV glycoprotein (GP)[6 7]. MARV GP is the viral transmembrane protein that binds to the target cell and interacts with the host CD209/DC-SIGN and CLEC4M/DC-SIGNR proteins to facilitate cell entry and subsequent viral replication[8 9]. Using Self-amplifying mRNA (saRNA) provide a key advantage in vaccines in comparison to conventional mRNA as it requires smaller does to achieve the same therapeutic effect. This is because saRNA contains self-replicating enzyme that allows a single strand of saRNA to copy itself inside the cell, producing a significantly higher and longer-lasting protein output (Figure 1)[10,11]. The saRNA approach is anticipated to induce an effective immune response and moreover, be dose sparing. This novel vaccine format is being used to develop an MVD vaccine using saRNA to translate the MARV GP transgene and an LNP formulation to facilitate delivery to the host cell [12].

Lipid nanoparticles (LNPs) have emerged as a versatile and rapid platform for delivering RNA, small molecule and peptides[13,14], offering unprecedented speed and versatility in antigen production. mRNA vaccines work by delivering synthetic viral antigen mRNA into host cells using lipid nanoparticles as a delivery system[15 16 17 18]. This innovative vaccine technology is being applied to provide pre-exposure prophylaxis for MVD and the related Ebola virus. For example, a synthetic mRNA modified using pseudo-uracil and delivered by a LNP has proven effective in raising antibodies against the Ebola glycoprotein providing protection against viral challenge in Guinea Pigs[19]. Similarly, an Ebola glycoprotein saRNA was shown to be protective in mice against Ebola virus infection[20]. More specifically, a modified mRNA targeting MARV GP also induced an immune response that provided protection against MARV in Guinea pigs[21]. A critical component of RNA vaccines, including saRNA vaccines, is the LNP delivery system[15 22]. LNPs facilitate vaccine delivery by: (1) encapsulating the RNA to increase stability by reducing enzymatic degradation; (2) facilitating delivery of the mRNA into the cytoplasm by being endocytosed into the endosomes; and (3) enhancing endosomal escape by causing endosomal membrane destabilization, thereby delivering the mRNA into the cytosol for translation by the ribosomes. Typically, LNPs are composed of four main components, namely ionizable lipids (which bind to RNA), helper phospholipids, cholesterol, and polyethylene glycol (PEG)-lipid conjugates (Figure 1). Additional functional materials can be added to the formulation to enhance the structural stability of the LNP or modulate its activity.

View Article Online
DOI: 10.1039/D6PM00134C

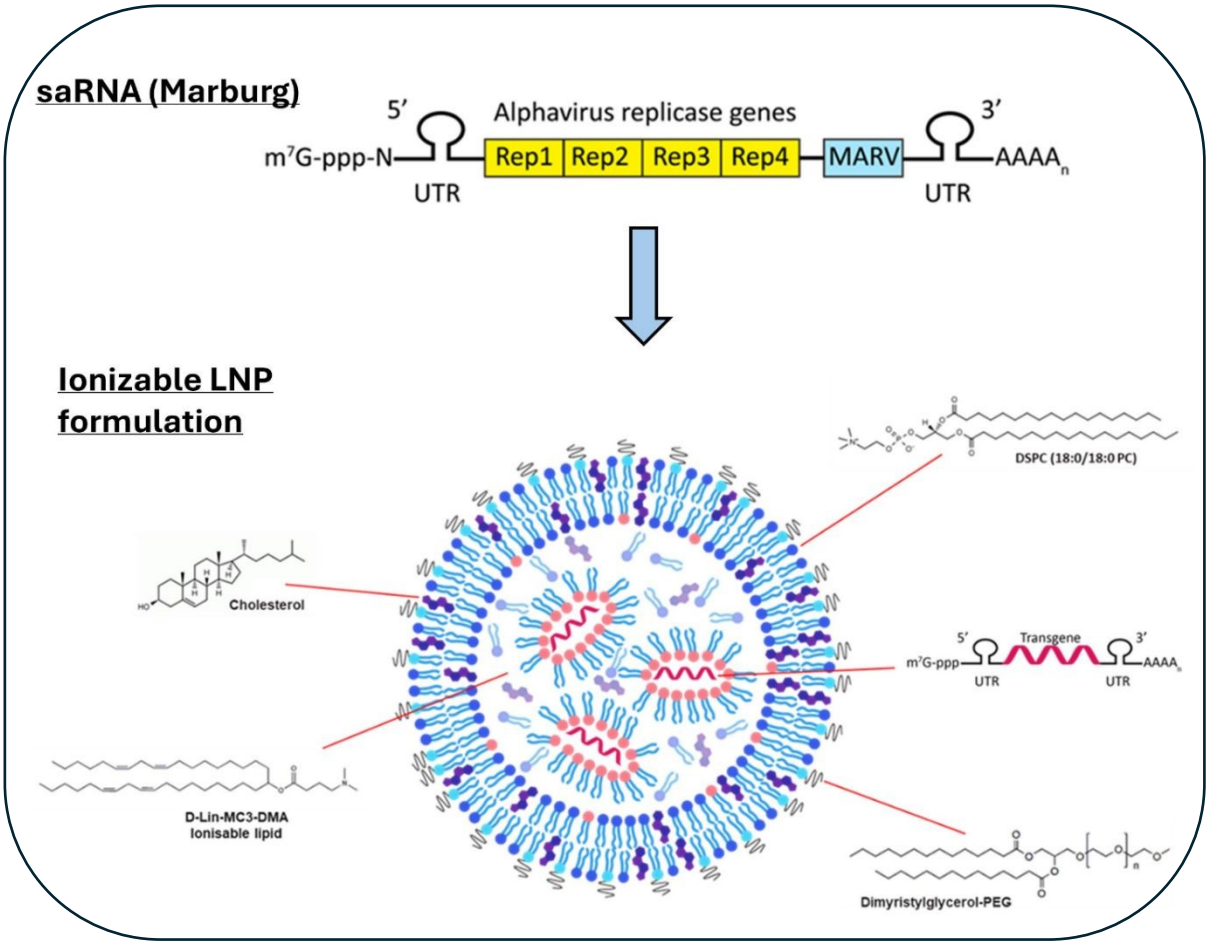

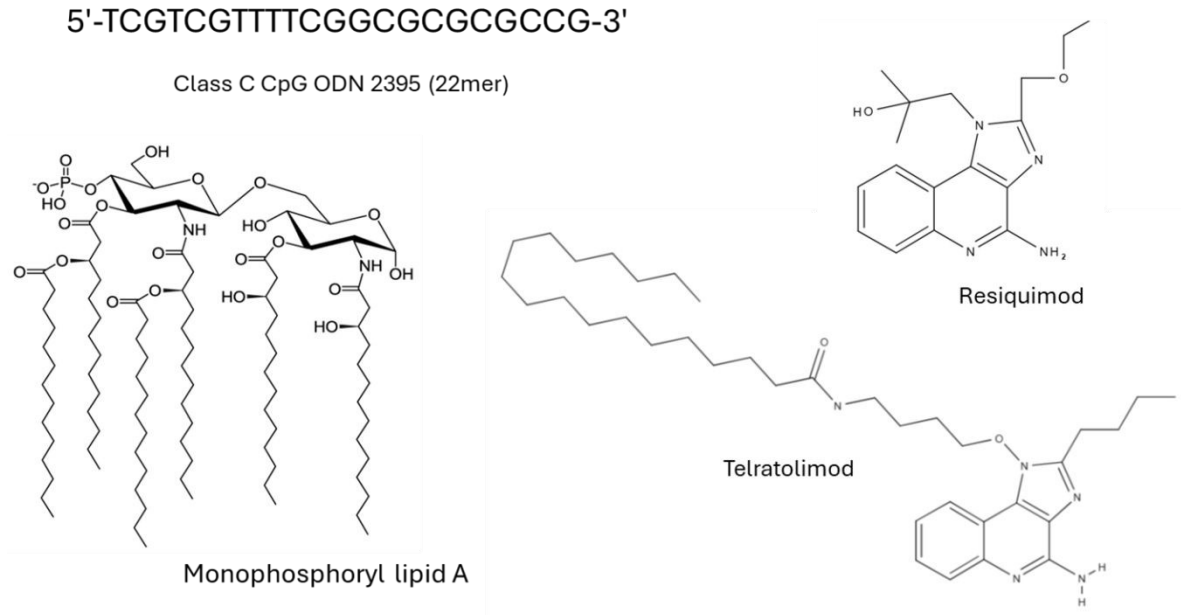

Figure 1: Schematic diagram of MARV GP saRNA-LNP vaccine formulation and the structures of the TLR agonists

View Article Online
DOI: 10.1039/D6PM00134C

In recent years, there has been significant development of vaccine adjuvants based on an increased understanding of the role of Pathogen-Associated Molecular Patterns (PAMPs) in activating the innate immune system. PAMPs are conserved molecular structures associated with pathogens which alert the immune system to microbial infection. Depending on their molecular structure, the PAMPs interact with Pattern Recognition Receptors (PRRs), which are mainly expressed by antigen-presenting cells (APCs) such as dendritic cells and macrophages, but they are also found in other immune and non-immune cells[23]. Based on an increased understanding of the role of PRRs in inducing the immune response, a series of agonists have been developed as vaccine adjuvants, particularly those targeting Toll-like Receptors (TLRs)[24,25].

Several studies have reported TLR agonists incorporated into RNA-LNPs enhances innate immunity while preserving protein expression[26 27] . TLRs are pattern recognition receptors critical for activating cell-mediated immune responses in the innate immune system. Specifically, TLR7/8 activation enhances T helper type 1 (Th1) immune responses through nuclear factor kappa B (NF-κB) signaling [28]. On the other hand, TLR9 agonists mimic bacterial and viral DNA to activate TLR9 which triggers MyD88 signaling pathway and drives B cell and dendritic cell to release pro-inflammatory cytokines[29]. The addition of TLR agonists to LNPs requires adjustments in nanoparticle composition to preserve efficient mRNA delivery [30].

This study had three primary aims: (1) to assess the immunogenicity of aMVD saRNA-LNP vaccine; (2) to evaluate LNP formulation modifications required to co-encapsulate a range of TLR agonists and (3) to assess the effects of the saRNA-LNP vaccine in the presence of the TLR agonists. In the first phase, a basic LNP formulation was produced comprising 10% 1,2-Distearoyl-sn-glycero-3-phosphocholine (DSPC), 38.5% cholesterol, 1.5% 1,2-Dimyristoyl-rac-glycero-3-methoxypolyethylene glycol-2000 (DMG-PEG2000), and 50% (6Z,9Z,28Z,31Z)-Heptatriaconta-6,9,28,31-tetraen-19-yl 4-(dimethylamino) butanoate (D-Lin-MC3-DMA) as the ionizable lipid. This ionizable lipid was selected as a gold standard benchmark lipid with relatively low inflammatory potential in comparison to other available ionizable lipids (e.g., SM102 & ALC-0315) that possess potent adjuvant properties on their own[31,32]. Production involved a microfluidic process, combining an acidic aqueous phase, containing the saRNA, and an ethanolic organic phase, containing the lipid components. With the co-encapsulation of TLR agonists, these were selected based on a range of physico-chemical properties, namely a small molecule imidazoquinoline TLR7 agonists (Resiquimod and Telratolimod), a lipopolysaccharide TLR4 agonist (MPLA) and a negatively charged oligonucleotide TLR9 agonist (CpG ODN) (Figure 2). These were also selected as they had previously been tested in man and shown to be effective adjuvants. MPLA and CpG oligonucleotides are present in licensed vaccines such as Cervarix™ human papilloma vaccine[33], Shingrix® herpes zoster vaccine[34] (both contain MPL®) and HEPLISAV-B® hepatitis B virus (HBV) vaccine (CpG 1018)[35]. While imidazoquinolines have only been tested in developmental vaccines, imiquimod has been used in Aldara® for the treatment of basal cell carcinoma, actinic keratosis and genital warts[23]. Because of their differing physico-chemical properties each TLR agonist required a unique LNP formulation to maintain efficient saRNA encapsulation.

Once formulated, we tested the basic saRNA-LNP vaccine and optimised TLR agonist formulations in mice, examining both B- and T-cell responses, to evaluate any impact on the anti-MARV immune response. Here, we report the immunogenicity of an MVD saRNA-LNP vaccine.

View Article Online
DOI: 10.1039/D6PM00134C

Additionally, we demonstrate differential effects of the TLR agonists on the B- and T-cell responses to the vaccine.

Materials and Methods

Materials

Dilinoleyl-methyl-4-dimethylaminobutyrate MC3 (DLin-MC3-DMA) (Cat.No. HY-112251), UltraPure™ DNase/RNase-Free Distilled Water and Ethanol (EtOH) was obtained from Fisher Scientific (Loughborough, UK). 1,2-Distearoyl-sn-glycero-3-phosphocholine (DSPC) (Cat.No. 850365P), 1,2-dimyristoyl-rac-glycero-3-methoxypolyethylene glycol-2000 (DMG-PEG 2000) (Cat.No. 880151P) and Monophosphoryl Lipid A (PHAD™) (MPLA PHAD™) (Cat.No. 699800) were purchased from Avanti Polar Lipids (Alabaster, AL, USA). Cholesterol (Cat.No. C8667), citric acid, sodium citrate tribasic dehydrate were acquired from Sigma-Aldrich (St Louis, MO, USA). Telratolimod (Cat.No. HY-109104) was purchased from Cambridge Bioscience (Cambridge, UK). CpG ODN, Class C (human/mouse) - TLR9 agonist (Cat.No. tlrl-2395) was sourced from InvivoGen (San Diego, USA). Phosphate-buffered saline (PBS) was acquired form Gibco@ (Cardiff, UK) Quant-it™ RiboGreen RNA Assay Kit, RiboGreen RNA Reagent, RediPlate™ 96 RiboGreen™ RNA Quantitation Kit, Quant-iT PicoGreen dsDNA Assay Kit were purchased from Fisher Scientific UK Ltd (Renfrew, UK). Kinetic-QCL™ Kinetic Chromogenic LAL kit was sourced from Lonza bioscience (Slough, UK). All solvents and other chemicals were of analytical (UPLC) grade, and Milli-Q-water was provided by an in-house system.

Methods

Plasmid construct and in vitro transcription of the saRNA

For the synthesis of the MARV GP saRNA a plasmid vector was produced. The saRNA comprised 9,829 nucleotides in length, encoding for two major components; the non-structural replicase proteins from VEEV epizootic Trinidad Donkey strain and the Marburg glycoprotein (GenBank accession number: QHD43416.1). The overall construct layout comprised of 5' Venezuelan Equine Encephalitis Virus (VEEV) nsP1–nsP4 replicase complex – VEEV subgenomic promoter – MARV GP ORF – 3′ UTR – Poly(A) tail. The plasmid was propagated in E. coli and linearized downstream of the poly(A) tail using a restriction enzyme that leaves a clean 3′ end. Manufacture of the saRNA was performed by in vitro transcription (IVT) by the RNA Centre of Excellence, CPI, Darlington, UK. SaRNA was generated from the linearised DNA template by in vitro transcription with co-transcriptional capping ($_{m7}$G(5')ppp(5')(2' OMeA)pU) (TriLink Biotechnologies, San Diego, USA) in the presence of nucleotide triphosphates (ATP, CTP, GTP, UTP) and Mg^{2+} ions. After transcription, the RNA was treated with DNase I to remove residual template DNA, and saRNA precipitated using Lithium Chloride. Finally, the saRNA was subject to buffer exchange by tangential flow filtration (TFF) into phosphate buffered saline and sterile filtered using 0.2um filters. Quality Control batch release testing demonstrated that the saRNA was within specifications.

View Article Online
DOI: 10.1039/D6PM00134C

Aqueous and organic phase preparation

The aqueous phase containing filtered buffer or saRNA or TLR9 agonist (CPG) with saRNA were prepared and kept on at 4 °C until microfluidic processing. The formulation buffer for the aqueous phase was made using DNase/RNase-Free Distilled Water to obtain 50 mM citrate buffer (pH 5.5) following by filtration with 0.2 µm filter. A stock solution of saRNA was diluted with formulation to 15 µg/mL which was later adjusted after microfluidic processing and purification. The organic phase containing either only essential lipids combination or TLR 7 agonist with lipid combination or TLR 4 with lipid combination were prepared separately. The lipid molar ratio of the LNPs was 10: 38.5: 50: 1.5% (Helper lipid: cholesterol: ionizable lipid: PEGylated lipid). The lipids were dissolved in ethanol and heated for 38 °C before injecting into the microfluidic device at a concentration of 8-10 mg/mL.

Manufacture and purification of the LNPs

Staggered herringbone micromixer obtained from Darwin Microfluidics connected to high precision syringe pumps from Harvard Apparatus (PHD Ultra™ HA3001). The ethanol-based organic phase contained the four component LNP mix with or without the corresponding lipid-based TLR agonists (MPLA or imidazoquinolines) and the citrate buffer-based aqueous phase with only saRNA or saRNA with TLR9 agonist CpG were fed through syringes into a microfluidics chip. The pumps were used to generate the flow in the micromixer at flow rate ratio (aqueous: organic phase) was set to 3:1 and total flow rate 4 mL/min. For purification by buffer exchange, the LNP sample in the original buffer was exchanged into PBS (pH 7.4) using 2 cycles of 30KD Amicon ultra centrifugal filter tubes. The centrifugation speed was set to 6000*g*. centrifugation time 10-20 minutes each cycle until 90% of the buffer was removed and replaced with the new buffer to the original sample volume.

Measuring critical quality attributes (CQAs)

Physicochemical properties

Size (Z-average diameter), polydispersity index (PDI) and zeta potential were measured using the Malvern Panalytical Zetasizer ZS and Zetasizer Ultra, using the ZS XPLORER V.1.3.2.2.7 software for data processing. Size and PDI were acquired via dynamic light scattering (DLS) function, using a measurement angle of 173° backscatter, and zeta potential was measured using voltage measurements in Zetasizer Cuvettes (DTS1070). To assess the impact of TLRs on particle charge, the LNPs were measured in citrate buffer (pH: 5.5) post-purification in PBS buffer (pH: 7.4). The dispersant refractive index and absorption were set to 1.335 and 1.02 cP, respectively for PBS, and 1.47 and 1.28 cP for citrate buffer.

saRNA and the adjuvants content

Encapsulation efficiency of saRNA was measured using the RiboGreen™ mRNA quantification assay kit according to the vender's protocol. Tris-EDTA (TE) buffer was used as the diluent in all steps of this assay. The fluorescent dye was used to measure the concentration of saRNA in the presence and absence of 1% Triton x which disrupt the structure of the LNPs. saRNA and ribosomal RNA standard curves were used in the assay. After 90 minutes of incubation at 37 °C, the fluorescence signal was read using Spectramax gemini microplate spectrofluorometer

View Article Online
DOI: 10.1039/D6PM00134C

(Molecular devices) 475–485 nm excitation and 525 nm emission wavelengths. SoftMax®Pro 7 v.7.0.3 software was used to process the data, and the encapsulation efficiency was calculated as follows:

$$EE\% = \frac{Total\ RNA - Free\ RNA}{Total\ RNA} * 100\%$$

Where total saRNA concentration was measured from the wells treated with 1% Triton x and free saRNA was measured from the wells with LNPs in only TE buffer. saRNA total content was measured using a calibration curve (Suppl Figure 2), which was later used to adjust dilution required to achieve the desired final concentration for animal testing.

Similar to RNA quantification, measuring the TLR9 agonist CPG in the corresponding formulation was also required. This was achieved by running Picogreen assay as CPG in essence is ssDNA. The procedure for Picogreen assay was as per Ribogreen that was described except for the use of Picogreen reagent. To prevent interference form RNA with picogreen RNAse was used to degrade saRNA in the wells before adding the Picogreen reagent. For TLR7 agonist (Telratolimod) encapsulation efficiency, LNPs were added to Zeba™ Spin desalting columns to remove any not incorporated Telratolimod. The concentration of before and after desalting was measured using Solo VPE λ_{max}: 248. To measure the MPLA PHAD™ content in the TLR4 agonist formulation, Kinetic-QCL™ Kinetic Chromogenic LAL Assay was used, and steps were followed as per the established manufacturer protocol.

Cryogenic transmission electron microscopy (cryo-TEM)

The manufactured saRNA-Lipid nanoparticle samples were maintained at manufacturing concentrations in pH 7.4 PBS. Holey carbon-coated copper grids were glow-charged using PELCO easiGlow at 15 mA for 30 seconds. 4 µL of each sample was blotted using an FEI Vitrobot (Thermo Fisher Scientific, UK). The humidity was set to 95% and temperature 4 °C, for 90 seconds and 5 force onto a holey carbon-coated copper gids followed by a second blotting of 4 µL (blotting time 10 seconds), then immediately plunged frozen in liquid ethane. Samples were kept in liquid nitrogen until imaging. CryoEM images were collected and processed using Glacios CryoEM (Thermo Fisher Scientific, UK) at 200 kV with a Falcon 4 direct electron detector.

Animal Care and Use Statement

All procedures in this study design are in compliance with the U.S. Department of Agriculture's (USDA) Animal Welfare Act (9 CFR Parts 1, 2, and 3); the Guide for the Care and Use of Laboratory Animals (Institute of Laboratory Animal Resources, National Academy Press, Washington, D.C., 2011); and the National Institutes of Health, Office of Laboratory Animal Welfare. Whenever possible, procedures in this study are designed to avoid or minimize discomfort, distress, and pain to animals. All animal procedures were approved by Labcorp, Early Development Laboratories Institutional Animal Care and Use Committee (IACUC) and Institutional Biosafety Committee (IBC). The Labcorp facility is accredited by the Associated for Assessment and Accreditation of Laboratory Animal Care (AAALAC).

Animals

Thirty-two (32) BALB/c female mice, approximately six (6) weeks of age were procured from Charles River Laboratories; Raleigh, North Carolina, USA.

View Article Online
DOI: 10.1039/D6PM00134C

Housing and Environment

Mice were placed in polypropylene mouse cages, six (6) mice per cage upon arrival. Each mouse cage contained Tekland Certified Diamond Soft T.7089C bedding with cardboard tubes for enrichment. All mice had access to food (Lab Diet 5001) and water, ad libitum. Complete change-out of mouse cages occurred at least once every week. The animal room had a photoperiod of 12 hours light, 12 hours dark, and temperature was maintained between 63°F to 77°F (17°C to 25°C), with a relative humidity of 50 ± 20% and at least 10 air changes per house. Animals were acclimated for 7 days prior to study initiation. During acclimation, mice were implanted with AVID RFID (Radio Frequency Identification Implant) in the nuchal area. Each implant encodes for a 9-digit number that was assigned to the Animal ID.

Daily Observations and Body Weights

All mice were observed for signs of morbidity and/or mortality at least once daily, according to standard operating procedures. Body weights were taken once on Day 0 as a baseline and once on Day 35 prior to termination.

Survival Blood Collections

Survival blood collections were taken on Day 0, prior to immunization, and Day 14. Prior to immunizations, each mouse cage containing all 6 mice from each respective group was placed in a biological safety cabinet (BSC). AVID RFID implants were scanned to verify identification number with the appropriate animal number and group. Once verified, mice were given 0.5% proparacaine hydrochloride ophthalmic solution in either the right or left eye, which lasts up to 1 hour. Mice were bled via the retro-orbital method. Approximately 200µL of whole blood was drawn into serum separator tubes (SST) per mouse. Animals were returned to their cages and observed for full recovery. Whole blood remained at room temperature in SST for at least 20 minutes before being spun in a centrifuge at 2000xg for 10 minutes. Serum was aliquoted in one bulk aliquot per animal and stored at -20°C or below until analyzed.

Test Article Preparation

On each day of immunization, test articles Empty LNP (Negative Control), lnpMARV, lnpMARV-Tel (TLR-7), lnpMARV-CpG (TLR-9), and lnpMARV -MPLA (TLR-4) were removed from -80°C ± 10°C freezers and thawed at room temperature. All surface areas inside the BSC and items within (including but not limited to pipettes, pipette tip cagees, racks, ice buckets, pens, zip-lock bags, and especially gloves) were treated with RNAse Zap (Sigma) or a similar product prior to and during handling of mRNA samples. 200µL of each test article was diluted with 300µL of sterile PBS. The material was mixed by pipetting up and down at least ten times. All prepared dilutions were maintained on ice packs during preparation. A volume of 50uL (0.2µg mRNA) of each test material was drawn up into 29G, 1.0mL insulin syringes to be transported to the animal room.

Immunizations

Prior to immunizations, all 6 mice from each respective group were placed in a BSC. AVID RFID implants were scanned to verify identification number with the appropriate animal number and group. 50uL injections were given intramuscularly in right quadriceps on Day 0 and left quadriceps on Day 21, ensuring avoidance of the sciatic nerve while dosing. Individual animals were returned to their home cage after dosing.

View Article Online
DOI: 10.1039/D6PM00134C

Injection Site Scoring

All mice had injection sites scored via the Modified Draize Scoring method for three days following each immunization (Days 1, 2, 3 and Days 22, 23, 24). Erythema Formation and Edema Formation were scored separate for each injection site.

Table 1: Modified Draize Scoring Chart: Erythema Formation

Score	Description
0	No Erythema
1	Very Slight Erythema (barely perceptible)
2	Well-Defined Erythema
3	Moderate Erythema
4	Severe Erythema (beet redness) to slight eschar formation

Table 2: Modified Draize Scoring Chart: Edema Formation

Score	Description
0	No Edema
1	Very Slight Edema (barely perceptible)
2	Slight Edema (edges of area well-defined by definite raising)
3	Moderate Edema (raised approximately 1 millimeter)
4	Severe Edema (raised more than 1 millimeter and extending beyond area of exposure)

Terminal Procedures

On Day 35, all animals were exsanguinated, terminated, and had spleens removed. Prior to terminal procedures, each mouse cage, containing all 6 mice from each respective group were placed in a BSC. Individual mice were picked up by the scruff or by the cupping method. AVID RFID implants were scanned to verify identification number with the appropriate animal number and group. Once verified, individual mice were placed in a CO_2 chamber. After cessation of breathing, mice were exsanguinated via jugular into SST for maximum volume. Each animal was reintroduced into the CO_2 chamber to verify complete euthanasia in accordance with approved protocols. Whole blood remained at room temperature in the SST for at least 20 minutes before being spun in a centrifuge at 2000xg for 10 minutes. Serum was aliquoted in one bulk aliquot per animal and stored at -20°C or below until analyzed.
Spleens were removed aseptically and placed into 5mL sterile tubes containing ~3.5mL CTL media (CTL, cat# CTLT-010) prior to being processed to splenocytes. Spleens were kept on ice packs until processing (which occurred on the same day).

Measurement of IgG, IgG1 and IgG2a Endpoint Titers via ELISA

Endpoint IgG, IgG1, and IgG2a titers in serum samples from immunized animals were measured using a standard in-house ELISA procedure. Each sample was analyzed separately for IgG, IgG1, and IgG2a titers. 96-well plates were coated by adding 100 µL of Marburg Virus Envelope Glycoprotein (The Native Antigen Company, cat# REC31934) at a concentration of 1.0 µg/mL per well and were incubated overnight at 2-8ºC. Plates were washed with wash buffer (1X PBS + 0.05% Tween 20) and 200 µL of blocking buffer (1X PBS + 3% BSA) was added to each well to prevent background reactivity. The plates were incubated at room temperature for 60±5 minutes and then washed with wash buffer.

View Article Online
DOI: 10.1039/D6PM00134C

The positive control (Mouse Monoclonal Anti-Marburg virus glycoprotein (MARV GP) IgG, purified (Alpha Diagnostic International, Cat #: MVGP13-M) IgG and IgG1 analysis only), negative control (pooled Day 0 sera) and serially diluted samples (serum processed from blood collected on study Days 0 and 35) were added to their designated wells at a volume of 50 µL/well, and plates were incubated at 37±2ºC for 60±5 minutes. After washing away unbound antibody, the Marburg Virus Envelope Glycoprotein specific antibody captured on the ELISA plates was detected by adding a HRP labeled anti-mouse IgG (Jackson ImmunoResearch, cat# 715-035-150), IgG1 (Fisher Scientific, cat# A10551), or IgG2a antibody (Fisher Scientific, cat# A10685) at 100 µL/well and incubating the plates for 60±5 minutes at room temperature. Plates were then washed and enzyme activity was measured with ABTS (2,2'-Azinobis [3-ethylbenzothiazoline-6-sulfonic acid]-diammonium salt, 100 µL/well). The plates were incubated for 30±2 minutes at room temperature, and absorbance was read at 415_{nm} with a reference at 570_{nm}.
A four-parameter equation (Y = ((A-D)/(1+(x/C)^B)) + D) was used to fit each titer curve using Gen5 version 3.08.01. The endpoint titers, or the reciprocal of the sample dilution at which the absorbance corresponds to a set cut point, were calculated by Gen5 at a cut point of 2 x average OD of assay diluent. The data displays all the variables (A: peak absorbance, B: Hill slope, C: 50% titer, or reciprocal of dilution and D: baseline absorbance) and their values for each titer curve. Geometric mean titer values were calculated using Microsoft Excel and Mann Whitney statistical analysis was performed using GraphPad Prism10.

Splenocyte Preparation for ELISpot

To determine whether the immune response induced by the vaccines is mediated through Interferon-γ (IFN-γ) and/or Interleukin-5 (IL-5), an ELISpot assay was run on splenocyte pools from the 30 immunized mice (groups 1-5). The spleens were individually homogenized in gentleMACS C tubes using the gentleMACS Octo Dissociator on program *m_spleen_04_01*. The homogenate was pelleted by centrifugation at 300xg for 8 minutes and the supernatant was poured off. The pellet was tapped out, and 1 mL of ACK lysis buffer (Gibco, cat# A10492-01) was added at room temperature to lyse the red blood cells. After 4 minutes, CTL media was added to neutralize the ACK lysing buffer. The cells were pelleted by centrifugation at 300xg for 8 minutes and the supernatant was poured off. The pellet was tapped out, and the cells were resuspended in 5 mL CTL medium + 1% Glutamax (Gibco, cat# 35050-061) + 1% P/S (Sigma, cat# P4333). The cells were passed through a 70 µm tissue sieve into a sterile 50 mL centrifuge tube and a 100 µL sample was taken for a cell count. Cell counts were performed using a Nexcelom Cellometer Auto 2000 and AO/PI viability dye (Nexcellom, cat# CS2-0106-5mL). The concentration for each sample was adjusted to $3x10^6$ cells/mL in 1 mL warm CTL medium + 1% Glutamax + 1% P/S. The samples were pooled in sterile 5 mL tubes by group by taking 0.5 mL from each sample at $3x10^6$ cells/mL for a total of 3 mL. The cells were maintained in a 37±2°C, 9±1% CO_2 humidified incubator until use.

Measurement of IFN-ɣ and IL-5 via ELISpot

The ELISpot assay was performed using a commercial kit (CTL, cat# mIFNgIL5-1M). The detailed kit procedure followed is available from the manufacturer. The day before the assay, the plates were treated with 70% ethanol, washed with PBS (Cytiva, cat# SH30028.03), and coated with Interferon-γ and Interleukin-5 capture antibody before being stored at 2-8°C overnight. The day

View Article Online
DOI: 10.1039/D6PM00134C

of the assay, the plates were washed with PBS. The Marburg virus PepMix (JPT, cat# PM-MARV-GPAng, 2 µg/mL) and ConA (Sigma, cat# C0412, 2 µg/mL) were prepared in CTL media, added to the appropriate wells at 100 µL/well, and incubated at 37°C, 9±1% CO_2 in a humidified incubator for at least 10 minutes. The cells adjusted to $3x10^6$ cells/mL and pooled by group were added to the appropriate wells at 100 µL/well ($3x10^5$ cells/well with 1 µg/mL stimulant) and incubated for 24 hours in a 37±2°C, 9±1% CO_2 humidified incubator.

After 24 hours, the plates were washed with PBS and 0.05% Tween-PBS (Tween - Fisher, cat# BP337-500). Anti-murine IFN-γ-FITC / IL-5-biotin detection was added to the plates at 80 µL/well and incubated at room temperature for two hours. The plates were washed with 0.05% Tween-PBS. Tertiary antibody (FITC-HRP / Strep-AP) was added to the plates at 80 µL/well and incubated at room temperature for one hour. The plates were washed with 0.05% Tween-PBS and Milli-Q water. Blue developer was added to the plates at 80 µL/well and incubated at room temperature for 15 minutes. The plates were washed with ELIX and Milli-Q water. Red developer was added to the plates at 80 µL/well and incubated at room temperature for 7 minutes. The plates were washed with ELIX water and left to dry at room temperature. Once dry, the plates were stored at 2-8°C and protected from light. Once dry, the plates were scanned using ImmunoSpot S6 Universal-V analyzer and analyzed using ImmunoSpot software version 7.0.34.0.

Results and discussion

Results

MARV saRNA-LNP Formulation

Having established the critical process parameters, the MARV GP saRNA was formulated in a standard four component LNP. A target 2µg/ml RNA content was selected based on prior work, which would provide a 0.2µg/100ul dose for the *in vivo* study[36]. Moreover, target values were adopted, comprising particle size of <200nm, polydispersity index (PDI) <0.2, and saRNA % encapsulation efficiency (%EE) of >80%. The lnpMARVs were then produced using a flow rate ratio (FRR) of 3:1 (aqueous: organic phase), a total flow rate (TFR) of 4mL/min, and 10mg/mL. Analysis of the lnpMARVs demonstrated that the CQAs were within the prescribed range (Figure 2 & Table 3). Additionally, empty LNPs were produced as a negative control using the same process and formulation, except for the absence of the RNA payload.

MARV saRNA-LNP co-formulation with TLR agonists

Having established the basic lnpMARV formulation, the next step was to evaluate the incorporation of each of the TLR agonists. As described above, the aim was to evaluate three distinct agonist moieties. Again, based on prior knowledge, the target dose for each TLR agonist was 200-500µg/mL with ≥80% %EE, while maintaining the >80% saRNA %EE. As each of the selected TLR agonist had different characteristics, the approach to co-formulation with the lnpMARV was different. MPLA, which contains several alkyl chains and was the most hydrophobic of the agonists, was initially thought to be able to incorporate into the LNP structure readily. However, the hydrophobicity of MPLA required an ethanolic solution containing 10% (v/v) DMSO, along with the lipid components, to achieve a 1mg/mL MPLA concentration. Incorporation

View Article Online
DOI: 10.1039/D6PM00134C

of the MPLA did not impact the microfluidic production of the MPLA MARV GP saRNA-LNPs (lnpMARV-MPLA), albeit it did result in a noticeably larger particle size (~180 nm) and a PDI value of 0.19, which was close to the prescribed acceptance value of 0.2 (Table 3). Similarly, the DMSO had no apparent effect upon LNP formation; moreover, following buffer exchange the DMSO concentration was <0.03%

The ZP revealed that the particles had a slightly higher negative charge in physiological buffer, which was attributed to the phosphate group of the MPLA moiety. %EE determination for the saRNA demonstrated ~93%, within the prescribed criterion. As MPLA is an endotoxin variant, to determine MPLA %EE, we used a limulus amebocyte lysate (LAL) assay, which indicated that 99% of the MPLA was incorporated into the LNPs. As the formulated lnpMARV-MPLA was within the acceptance criteria, further optimisation was not considered at this stage.

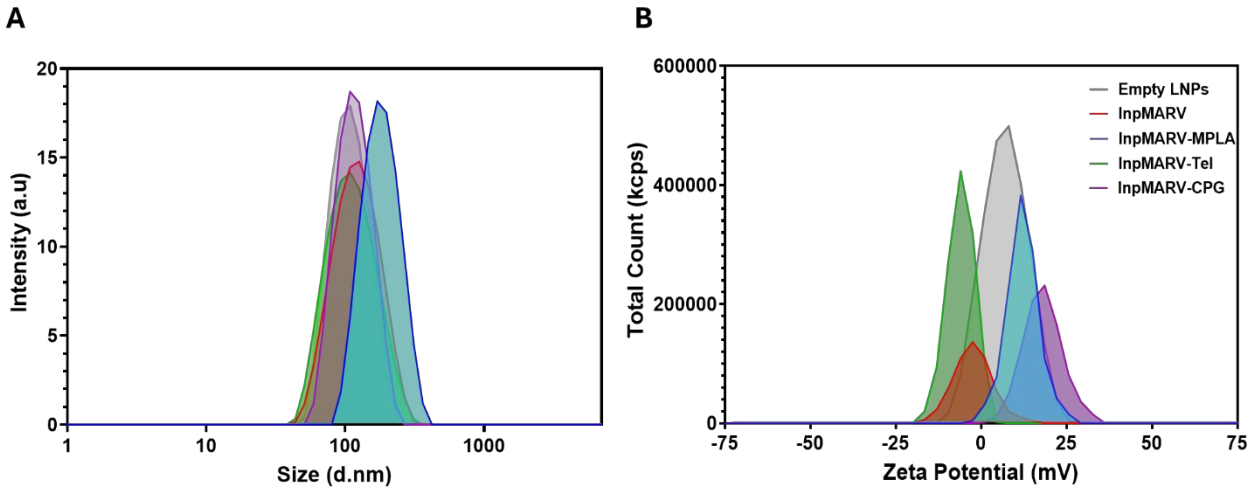

Figure 2. (A) particle size distribution of LNPs (B) Zeta potential distribution at pH 5.5 (when ionizable lipid is charged).

Table 3: Critical Quality Attributes of lnpMARV, empty and LNP TLR agonist lnpMARV formulations (n=3 ± sd).

LNP Formulation	*Particle Size (nm)*	*PDI*	*Zeta Potential (mV) in pH 5.5*	*Zeta Potential (mV) in pH 7.2*	*saRNA Encapsulation Efficiency %*	*Adjuvant Incorporation Efficiency%*
Empty LNPs	130 ± 4.9	0.11 ±	5.75 ± 0.6	-2.77 ± 0.7	N/A	N/A
lnpMARV	111 ± 3.1	0.12 ±	7.74 ± 1.1	-2.16 ± 0.5	95.7 ±1	N/A
lnpMARV-MPLA	181 ± 8.2	0.19	11.2 ±1.3	-5.1 ± 0.9	93 ±2.1	99% ± 0.4
lnpMARV-Tel	109 ± 7.3	0.13	7.9 ± 0.9	-2.3 ± 0.4	90 ±3.3	82% ± 2.0
lnpMARV-CpG	110 ± 7.9	0.08	9.1 ± 1.0	-5.0 ± 0.3	90 ±1.3	91% ± 2.1

Co-formulation of CpG ODN 2395, required the incorporation of a highly negatively charged moiety into the LNP, without impairing saRNA encapsulation. Formulation parameters were determine using a DoE approach. Based on a risk assessment of the critical formulation

View Article Online
DOI: 10.1039/D6PM00134C

parameters, total lipid concentration (6-10 mg/mL); total nucleic acid concentration (200-500µg/mL) and pH of the acidic phase (pH4-6) were evaluated in a 2-level, 3-factor full factorial (Suppl. Table 1). For the DoE, polyA was used as a surrogate for saRNA. The CQAs were determined as endpoints for the study. This DoE formulation optimization for nucleic acid load identified total lipid and nucleic acid concentration as the statistically significant factors for RNA %EE (Suppl. Table 1 & Figure 1). With this LNP formulation, the maximal nucleic acid load was determined to be 325µg/mL for 10mg/mL total lipid concentration; however, to keep within a safe margin, it was decided to limit the CpG concentration to 200µg/mL. Using the optimised formulation parameters, CpG ODN 2395 saRNA-LNPs (lnpMARV-CpG) were produced, the CQAs determined, and the resultant LNPs were within the prescribed target: structurally, the LNP was 110nm in size with a PDI of 0.08 and a ZP of -5.03mV (Table 3). CpG %EE and saRNA %EE were determined using picogreen and ribogreen, respectively. By both parameters, the percentage of EE was ≥90%. One issue with using picogreen and ribogreen assays to determine the saRNA and DNA levels, respectively, is the potential for DNA interference in the picogreen assay to provide a false saRNA reading, particularly due to the high concentration of CpG compared with saRNA. To confirm that saRNA levels had achieved the >80% target, the picogreen assay was repeated, including incubation with DNase (RNase-free), to hydrolyse the CpG. In the absence of DNase, picogreen repeated the saRNA %EE value of 95%, whereas when incubated with the DNase, the value was 99%, confirming effective encapsulation of the saRNA.

The final TLR agonist to be co-formulated was resiquimod, a moderately lipophilic small molecule drug (logP of 1.72). The initial assumption was that the hydrophobicity of the molecule would be sufficient to enable its readily incorporation into the LNP lipid structure, thereby meeting the target of>80%. Preliminary formulations with resiquimod achieved a %EE of 88%; however, when co-formulated with polyA or saRNA, this resulted in a marked drop in %EE, with values of around 51% (Figure 3). As it was considered that increasing the hydrophobicity of the basic imidazoquinoline molecule would increase encapsulation, an alkylated imidazoquinoline, Telratolimod (Tel), was also tested (Figure 2). One possible explanation for the difference in adjuvant encapsulation efficiency between Resiquimod and Telratolimod is that the structure of the latter enables more rapid integration into the lipid mixture during LNP-RNA assembly. In contrast, a significant amount of Resiquimod remains in the ethanolic solution outside the assembled LNPs and is subsequently removed during purification. In the presence of RNA, complexation between ionizable lipids and nucleic acids promotes rapid assembly and stabilization of LNPs, leaving less time for hydrophobic small molecules such as Resiquimod to become entrapped within the LNP structure. A direct comparison of LNPs formulated respectively with Telratolimod and Resiquimod (both at 200µg/mL) demonstrated that Telratolimod %EE was significantly higher than Resiquimod in the LNP formulations ($p<0.001$) (Figure 3). The % EE of the saRNA was >90% irrespective of the TLR7 Telratolimod agonist (Table 3).

View Article Online
DOI: 10.1039/D6PM00134C

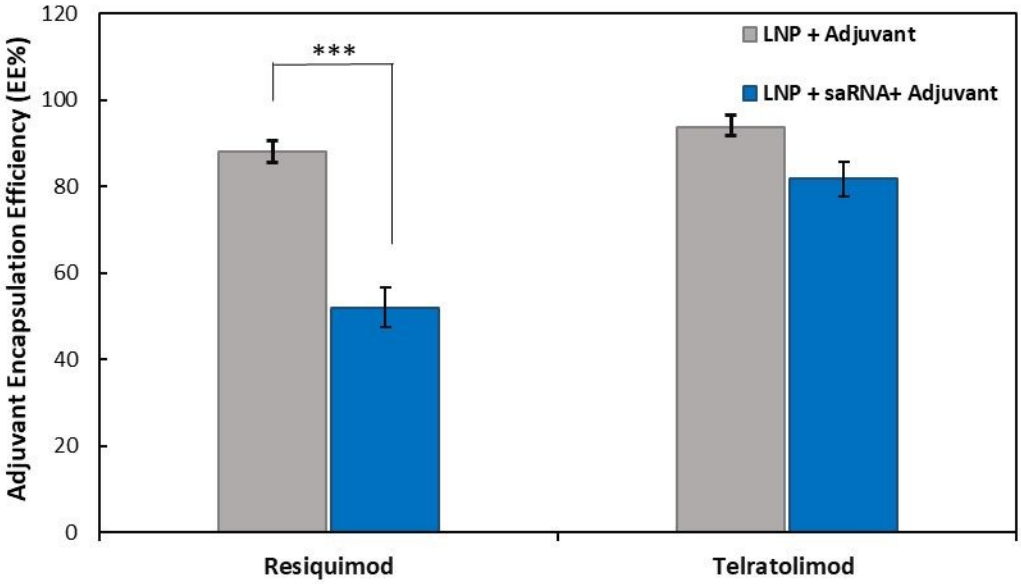

*Figure 3. %EE for TLR7 agonist forms in in the presence or absence of RNA. saRNA-LNP vaccine formulation. Telratolimod or Resiquimod incorporated with LNPs or with (blue) or without (gray) saRNA. (*** = $p < 0.001$)*

Having determined that Telratolimod resulted in increased %EE, it was selected as the TLR 7 agonist for LNP formulation. Tel saRNA-LNPs (lnpMARV-Tel) were produced using the optimised formulation parameters and the CQAs were determined. The resultant LNPs were within the target; structurally the LNP was 109nm in size with a PDI of 0.13 and a ZP of -2.25mV (Table 3).

To assess the stability of formulated LNPs at 2-8^{o}C, a stability study was performed. Using DLS for particle size analysis, LNP particle size was seen to be stable for up to 28 days when stored at 2-8^{o}C, for the lnpMARV and the TLR agonist formulations (Table 4A). More extended time periods resulted in a marked increase in particle size for lnpMARV-Tel, although not for the other formulations, which were stable over the 45-day test period. In a second study to evaluate freeze/thaw, formulated LNPs were aliquoted and frozen at -80^{o}C (intended storage condition) immediately following production. Two cycles of freeze-thaw at -80^{o}C were evaluated (Figure 4). With freeze-thaw, lnpMARV showed a progressive increase in particle size with each cycle, although after two cycles was still within the 200nm particle size acceptance target. The other formulations demonstrated no increase in particle size with the two cycles of freeze-thaw, except for lnpMARV-Tel, which showed a marked increase in size, exceeding the 200nm target. The entrapment of Telratolimod in lnpMARV-Tel formulation resulted in vacuoles in the LNP structure that are buffer filled. This would impact LNP stability at 4^{o}C and make them susceptible to ice crystal formation during freezing leading to aggregation.

View Article Online
DOI: 10.1039/D6PM00134C

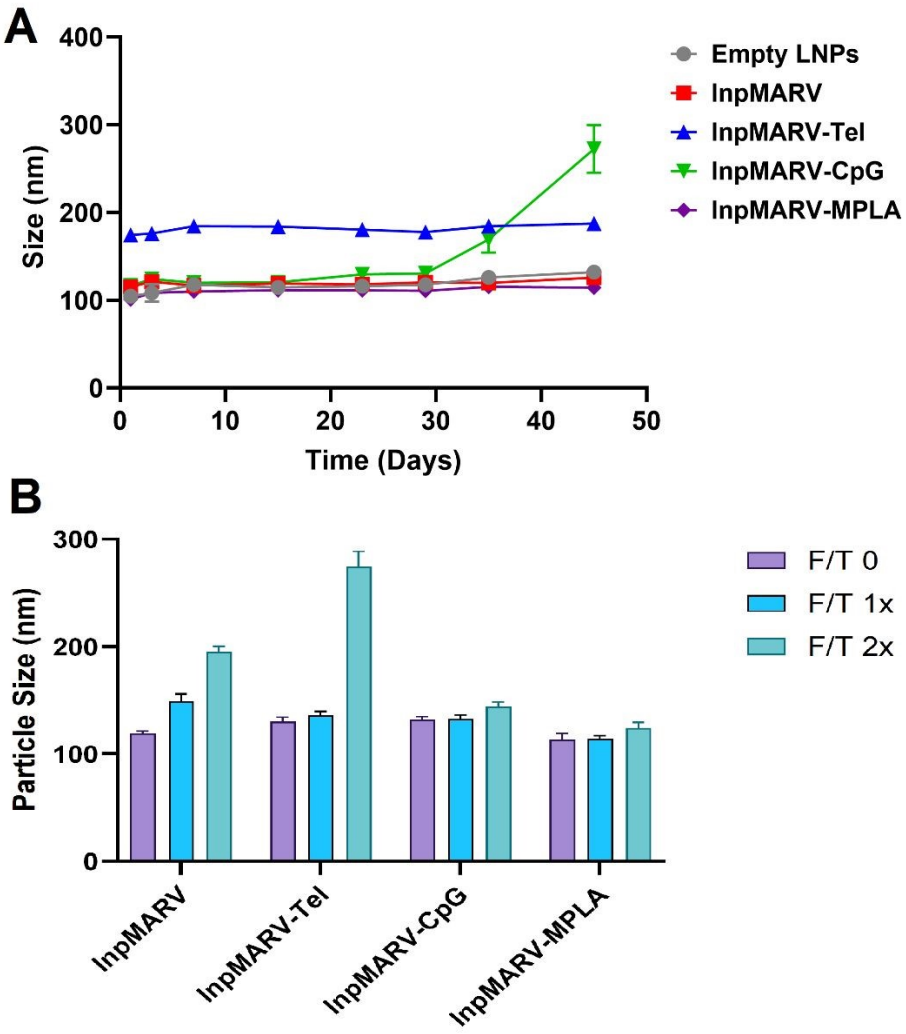

Figure 4: LNP particle size stability study showing storage at 2-8°C (A) and the impact of freeze-thaw cycles (B).

LNP Morphology

To determine the morphology of the LNPs, cryogenic transmission electron microscopy (cryoEM) was performed and revealed that the LNPs were consistent with general LNP morphology, namely an outer shell layer, generally with a dark homogenous core. When comparing the InpMARVs with the empty LNPs, the former appeared have more pronounced grainy core, potentially reflecting the saRNA payload (Figure 5). In line with the DLS size analysis, the InpMARV-MPLAs were round and visibly larger than the InpMARVs. While the outer lipid layer appeared to be of similar thickness, the increased size of the InpMARV-MPLA appeared to be due to a larger homogenous core. InpMARV-CpG demonstrated a similar morphology to that of the InpMARV,

View Article Online
DOI: 10.1039/D6PM00134C

with the noticeable exception that blebbing was occurring in some of the LNPs, as evident from low density vacuoles located between the outer layer and dense inner core (Figure 5). Interestingly, low-density vacuoles were also observed with the lnpMARV-Tel; however, these were distributed within the central core of the LNPs (Figure 5).

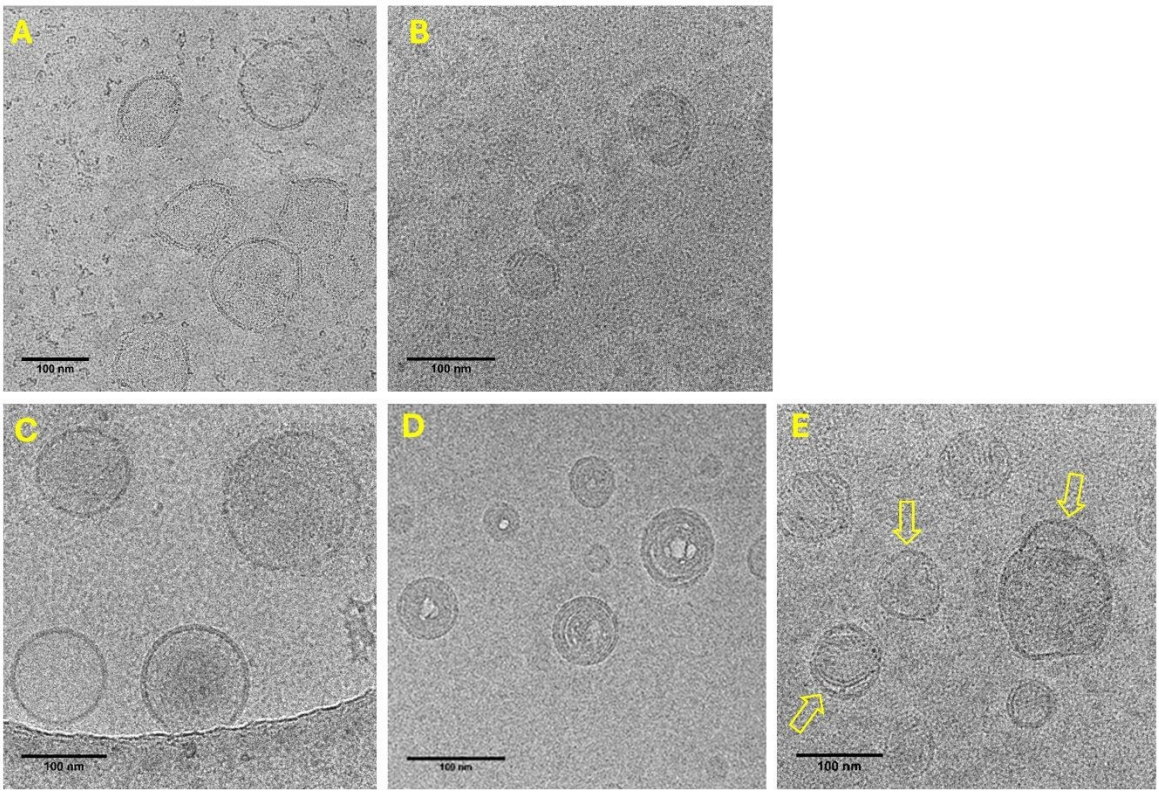

Figure 5: Cryogenic transmission electron microscopy of LNPs with DLin-MC3-DMA as the ionisable lipid in PBS pH 7.4. Images acquired show: (A) Empty (free) LNPs, (B) lnpMARV,(C) lnpMARV-MPLA, (D) lnpMARV-Tel and (E) lnpMARV-CpG. The yellow arrows indicate blebbing.

In vivo study

In vivo testing was performed using BALB/c mice with a prime-boost regimen to determine the relative effects of the TLR agonist formulations compared to the basic MARV saRNA-LNP formulation. An empty RNA-free LNP formulation comprising the same lipid components was used as a negative control. Based on prior knowledge of similar developmental LNP vaccines, a 0.2 µg saRNA dose was used (100 µg/mouse). This dose was intended to produce a suboptimal response, allowing for the detection of any TLR agonist modulation of the immune response. Similarly, a 20µg dose was used for each TLR agonist, and both B- and T-cell responses were assessed.

Following intramuscular immunisation, daily observations of the mice were performed along with injection site observations for three days post-immunisation. All animals remained bright, alert, and responsive (BAR) throughout the study. No animals exhibited any adverse reactions to their

View Article Online
DOI: 10.1039/D6PM00134C

respective test articles, and only minor injection reactions were seen with the primary immunisation. With empty LNPs, one animal exhibited very slight erythema, visible only on Day 1. Similarly, with lnpMARV, one animal had very slight erythema and edema on Day 1 and Day 2, which subsided by Day 3. For the TLR agonist formulations, very slight erythema and edema were seen with lnpMARV-CpG but subsided by Day 2 and for lnpMARV-MPLA one animal in Group 2 (MARV mRNA-LNP) had very slight erythema and edema on Day 1 and very slight edema on Day 2, but subsided by Day 3, although these had subsided by Day 2 and Day 3, respectively. There were no injection site reactions seen after the boost immunization (Suppl. Table 2). Overall, there were minimal immunogenic responses to the formulations, and no real differences between them.

B-cell Response

The humoral immune response following immunisation with the lnpMARV was evaluated at Day 35 by determining the levels of anti-MARV GP IgG in the sera via ELISA. At 0.2μg saRNA dose, the control lnpMARV demonstrated a statistically significant increase in anti-MARV GP IgG compared to an equivalent dose of empty LNPs and sterile PBS injection ($p < 0.05$) (Figure 6 & Suppl. Table 3); thereby demonstrating a specific B-cell response. The 0.2μg dose was sufficiently sub-maximal to assess potential enhancement and inhibition of the anti-MARV IgG response.

The lnpMARV-MPLA formulation demonstrated a statistically significant increase in response involving the TLR4 agonist compared to the standard lnpMARV formulation ($p<0.05$) (Suppl Table 3). In contrast, the lnpMARV-CpG formulation appeared to reduce anti-MARV IgG serum titres, although this did not reach statistical signifigance, while lnpMARV-Tel induced similar responses to lnpMARV. To evaluate the type of immune response stimulated by the different lnpMARV formulations, IgG subtype analysis was performed on the MARV IgG response. IgG1 and IgG2a titres were each determined by ELISA and the IgG1/IgG2a ratio was evaluated. No significant increase in IgG1 levels was detected between lnpMARV and the TLR agonist-containing vaccines (Figure 6A & Suppl. Table 4). Similarly, no significant difference was observed in IgG2a levels between lnpMARV and those containing the TLR agonists (Figure 6B & Suppl. Table 5). Interestingly, the IgG1/IgG2a ratio for each of the lnpMARV indicated that the induced immune response was predominantly Th2 (Figure 6C & Suppl. Table 6), representative of humoral immunity and allergic reactions, as opposed to cell-mediated immunity.

View Article Online
DOI: 10.1039/D6PM00134C

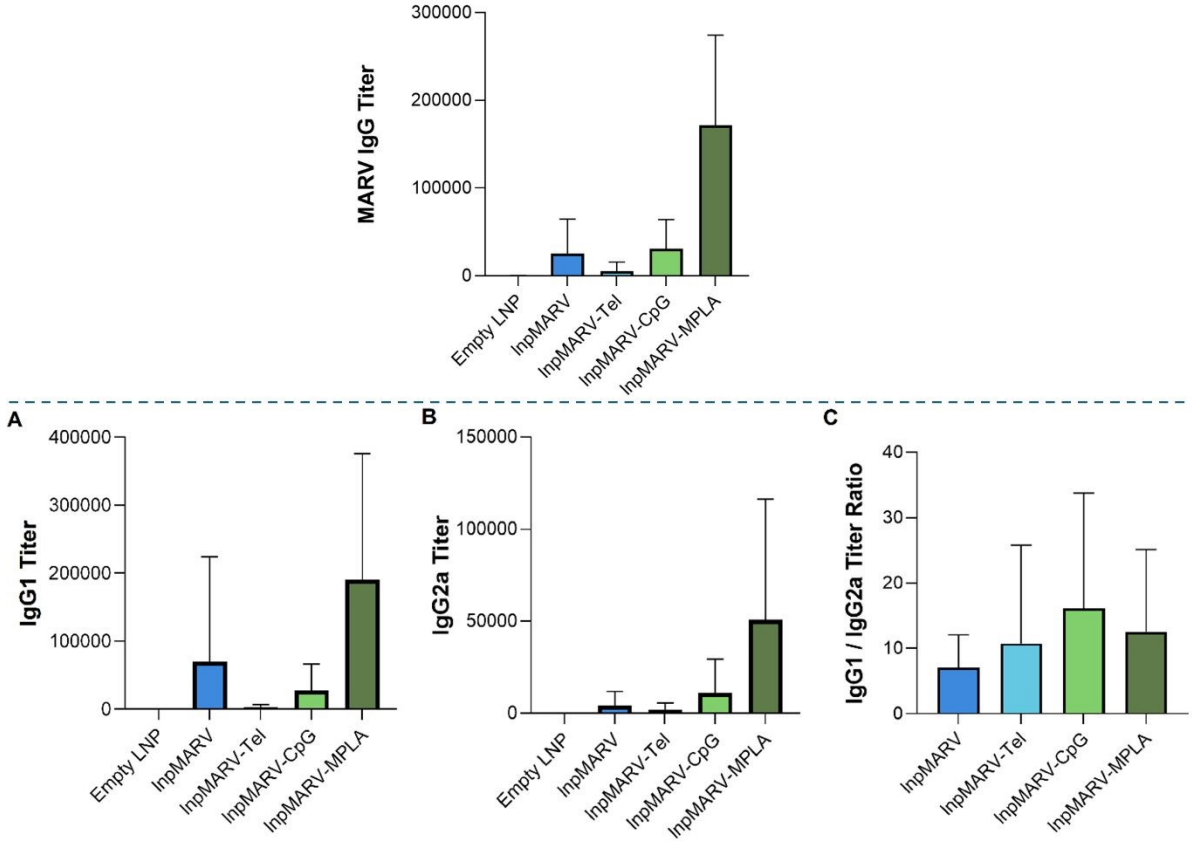

Figure 6: Upper part shows mouse sera anti-MARV IgG titres were determined using ELISA following immunization with InpMARVs ± co-formulation with TLR agonists. Sera was analysed on Day 35. Lower part shows anti-MARV IgG subtyping by ELISA to determine IgG1 (A), IgG2a (B) and IgG1/IgG2a ratio (C).

T-cell Responses

To evaluate the T-cell responses, the spleens were removed and the splenocytes were isolated and used for further analysis. Following stimulation with a MARV GP peptide mix, the level of IFN-γ and IL-5 producing T-cells was determined using a combined of IFN-γ / IL-5 ELISpot assay. A statistically significant activation of IFN-γ positive T-cells with InpMARV compared to empty LNPs was seen ($p<0.0001$) (Figure 7A, 8C & Suppl. Table 7). Moreover, the IFN-γ T-cell response was inhibited by InpMARV-MPLA ($p<0.002$), and particularly by InpMARV-Tel ($p<0.0001$); however, was not significantly decreased with the InpMARV-CpG. With the ELISpot analysis, the levels of IL-5 positive T-cells were very low, making interpretation of the data problematic. None of the MARV formulations demonstrated stimulation of IL-5 positive T-cells compared to background levels generated by empty LNPs (Suppl. Figure 3, 8C & Suppl. Table 8). Indeed, InpMARV-CpG and InpMARV-Tel both significantly inhibited IL-5 positive T-cells ($p<0.05$); moreover, with InpMARV-Tel ELISpot IL-5 positive T-cells were barely detectable ($p<0.05$). While the findings look interesting, due to the low numbers involved, further confirmation is required.

View Article Online
DOI: 10.1039/D6PM00134C

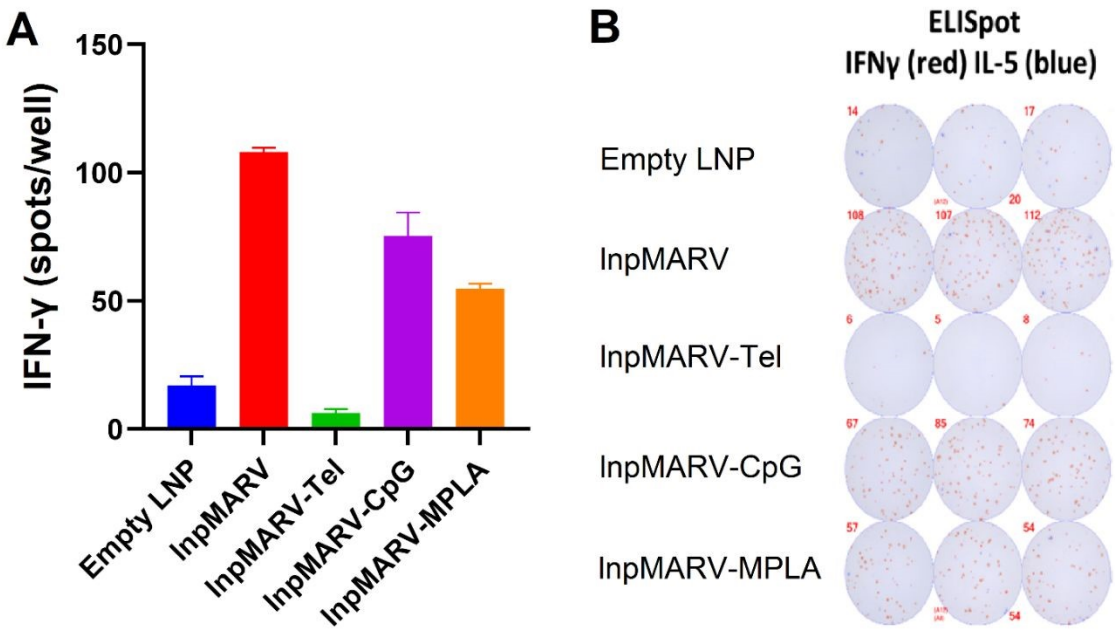

Figure 7: ELISpot analysis of IFN-γ and IL-5 levels in mouse splenocytes following stimulation with Marburg virus peptide mixture, showing the spots/well for IFN-γ (A), the ELISpot images (B). Splenocytes were analysed on Day 35.

View Article Online
DOI: 10.1039/D6PM00134C

Discussion

Having established the basic lnpMARV vaccine, the next step was formulation modification with the TLR agonists. We purposefully selected three structurally different TLR agonists in exploring the formulation space for incorporating additional agents into the LNPs. MPLA and CpG oligonucleotides were chosen as they represented a hydrophobic agonist and a highly charged hydrophilic agonist, respectively. Each TLR agonist posed distinct formulation challenges which were addressed in this study. With the CpG ODN, the challenge was one of capacity of the ionizable lipid to bind the nucleic acid load. While the content of saRNA was relatively low at 2ug/ml, the issue was whether a suitable dose of CpG ODN could be accommodated by the ionizable lipid in the nanoparticle. Another consideration is whether the excess load of CpG ODN would compete with saRNA for complexation with the D-Lin-MC3-DMA, thereby reducing the saRNA %EE. Formulation at 2ug/ml saRNA and 200ug/ml CpG ODN resulted in >90%EE for both nucleic acids. The results demonstrated that saRNA was not being displaced by the CpG ODN. Formulation with CpG ODN did not affect particle size or PDI, although it resulted in a more negatively charged particle, resulting from the increased nucleic acid load. CryoEM revealed the standard LNP morphology, outer bilayer and granular core. Where the morphology did differ from that of the lnpMARV was the evidence of blebbing in some of the LNPs, where low-density vacuoles were seen between the bilayer and the dense core. Such blebbing has previously been reported[37 38 39 40].

MPLA, comprising several acyl groups, was readily incorporated into the lnpMARV at 200ug/mL, along with efficient encapsulation of the saRNA of ≥90%. Going forward, potential options to use more aqueous/ethanol soluble TLR-4 agonists such as E6020[41,42] to avoid the addition of small percentage of DMSO during MPLA solubilization. The interesting feature of the lnpMARV-MPLA formulation was the increased particle size and PDI, albeit still within the target criteria. The increased particle size was also evident in the cryoEM images. While the bilayer was still apparent, the dense core region was enlarged compared to the lnpMARV particles. We speculate that the majority of the MPLA was incorporated into the DSPC/cholesterol bilayer, causing the bilayer expansion. Zeta potential revealed the lnpMARV-MPLA to be more negatively charged than the lnpMARV, consistent with the MPLA phosphate group being exposed to the solvent, where it can interact with the TLR4/MD2 receptor. Nevertheless, it is not possible to discount some localization of MPLA within the core, with the phosphate groups interacting with the D-Lin-MC3-DMA.

The third type of modified lnpMARV evaluated incorporated a small-molecule TLR7 agonist. Improved TLR7 encapsulation efficiency (%EE) was achieved using Telratolimod, a TLR7 agonist containing both butyl and octadecanyl modifications on the imidazoquinoline structure. Encapsulation of Telratolimod did not significantly alter particle size, size distribution, or zeta potential; however, notable changes in LNP morphology were observed. Structurally, the LNPs consistently displayed an outer bilayer surrounding a dense core, with low-density vacuoles present within the core region in a subset of particles. This vacuolization differed from the blebbing observed in the LNP-MPLA formulation, which occurred between the bilayer and the core, as the vacuoles appeared localized within the center of the core. These observations suggest that Telratolimod is predominantly localized within the core, where it may interact with saRNA and/or

View Article Online
DOI: 10.1039/D6PM00134C

D-Lin-MC3-DMA, potentially contributing to the reduced saRNA encapsulation, release or endosomal escape. Further structural studies are required to confirm the localization of the agonists within the LNPs. An important consideration for these agonist-containing formulations is the accessibility of the agonist to its target receptor, including whether the agonist is released from the particle or directly interacts with the receptor while associated with the LNP (See below).

The second phase of the study was to evaluate the various lnpMARV formulations for potency using a mouse model and evaluating both B- and T-cell responses. The BALB/c mouse was selected as the animal model as it is a well-established model for MVD[43,44]. A saRNA dose of 0.2ug was selected with the aim of producing a sub-maximal immune response, to enable the evaluation of the TLR agonists. The lnpMARV formulation induced a significant anti-MARV IgG response. Analysis of the IgG1/IgG2a subtype ratio indicated that the immune response was predominantly Th2-biased, consistent with a primarily humoral immune response. The Th2 skewing observed against a viral antigen may reflect the inherent immunological phenotype of BALB/c mice, which are predisposed toward Th2-type responses [45–47]. T-cell responses were assessed using isolated splenocytes stimulated with a MARV GP peptide pool, followed by combined IFN-γ/IL-5 ELISpot analysis. The lnpMARV formulation stimulated IFN-γ-producing T cells in response to peptide stimulation, indicating induction of an antiviral cell-mediated immune response. Collectively, these findings demonstrate that lnpMARV can induce both humoral and cellular immune responses in BALB/c mice and may have potential as a vaccine platform for MVD.

Co-formulation of lnpMARV with TLR agonists produced differential effects on the anti-MARV IgG response. Incorporation of the TLR4 agonist MPLA resulted in a modest but statistically significant ~4-fold increase in anti-MARV IgG titres. In contrast, lnpMARV-CpG and lnpMARV-Tel did not significantly increase anti-MARV IgG levels relative to lnpMARV alone and were significantly reduced compared with lnpMARV-MPLA. Notably, lnpMARV-Tel induced particularly low anti-MARV IgG levels relative to lnpMARV, suggesting a potential inhibitory effect, although this did not reach statistical significance. With respect to IFN-γ-positive T-cell responses, incorporation of the TLR agonists either had no significant effect (CpG) or reduced the response (MPLA and Telratolimod) relative to lnpMARV alone. Although these TLR agonists are generally associated with promotion of Th1-type immunity, this effect was not observed in the present study. While lnpMARV-MPLA significantly increased IgG2a levels compared with lnpMARV alone, the overall IgG1/IgG2a ratio was not significantly altered.

The mechanistic understanding of why a differential response was observed with the TLR agonists requires further investigation. While intramuscular administered mRNA-LNP vaccines will result in uptake and transgene expression in muscle cells, mainly monocytes and dendritic cells translated the mRNA and upregulated key co-stimulatory receptors (CD80 and CD86)[48]. Dendritic cells are known to express TLR4, TLR7 and TLR9; moreover all three TLR agonists are known to activate B- and T-cell responses by the Type 1 interferon response (Figure 8)[49,50], hence any observed differences may reflect the physico-chemical nature of the LNPs, such as lipid components, particle charge, size, shape and surface components[48,51,52]; including how the particle presents the agonists to their respective receptors. In part this may involve differences in cellular uptake and saRNA endosomal escape by the target antibody presenting cells, depending

View Article Online
DOI: 10.1039/D6PM00134C

on how the agonists affect the LNP structure and the subsequent interaction with the plasma and endosomal membranes. Our data indicates that with MPLA, the agonist is located within the surface layer of the LNP and hence may directly interact with TLR4, which is located in the cell plasma membrane. In contrast, as TLR7 and TLR9 are located in the endosome[50], for activation the lnpMARV-Tel and lnpMARV-CpG need to be endocytosed to gain access to their respective receptors. Additionally, once in the endosome, breakdown of the LNP structure presumably is required to release the agonists to bind to their receptors. With lnpMARV-CpG, the release of the CpG, along with that of the saRNA, would be facilitated by the acidification of the endosome. Endosomal acidification protonates the ionisable lipid, making it positively charged, resulting in disruptive interactions with negatively charged endosomal membrane lipids, modification of lipid phase behaviour, and ultimately a breakdown in the LNP structure with the release of mRNA into the cytosol[53]. Interestingly, the disruption of endosomal trafficking has been shown to diminish TLR9 induced Type 1 interferon expression in dendritic cells[54], which may in part account for the lack of a significant effect with this agonist. For lnpMARV-Tel this disruption of LNP structure may simply allow diffusion from the degrading LNP within the endosome, whereby it can interact with TLR7. Furthermore, the acidification is required to activate TLR7 and disruption of the endosomal maturation has been shown to result in TLR7 hyper-responsiveness and an enhanced Type 1 interferon response[55]. Such a mechanism could explain the lnpMARV-Tel inhibition of the IFNγ T-cell response.

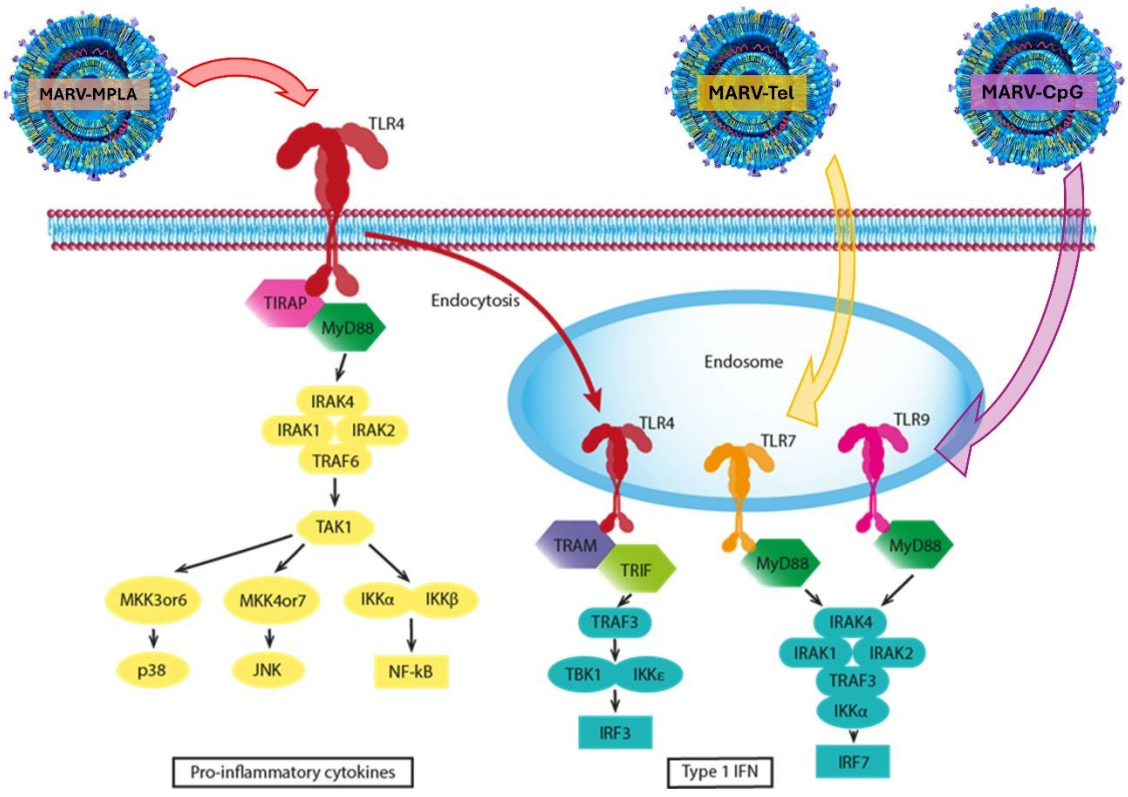

Figure 8: Schematic diagram showing the activation pathways of TLR4, TLR7 and TLR9.

View Article Online
DOI: 10.1039/D6PM00134C

Conclusion

In summary, this study demonstrates the successful formulation of a self-amplifying mRNA (saRNA) lipid nanoparticle (LNP) vaccine targeting the Marburg virus glycoprotein (MARV GP) using an advanced microfluidic process. While the base saRNA-LNP platform proved highly stable, immunogenic, and capable of driving strong anti-MARV IgG titers and IFN-\gamma expressing T-cell responses in a mouse model, the integration of distinct Toll-like Receptor (TLR) agonists yielded highly differential outcomes. Due to the vastly different molecular characteristics of the adjuvants—ranging from the highly lipophilic MPLA to the highly charged CpG ODN and the small molecule imidazoquinoline (Telratolimod)—tailored processing modifications were required, directly impacting the resulting physicochemical characteristics and morphology of the LNPs. Immunologically, the encapsulation of these agonists revealed that co-formulation is not universally beneficial. The TLR4 agonist MPLA successfully augmented humoral defenses by promoting anti-MARV IgG titers. Notably, while certain amine headgroups of ionizable lipids can inherently activate TLR4, the D-Lin-MC3-DMA lipid used in this study was determined to be immunologically inert and unlikely to have contributed to this specific MPLA boost [56]. This suggests that the strategic selection of alternative, immunoactive ionizable lipids could further enhance future TLR4-targeted responses. Conversely, co-formulations with CpG (TLR9) and Telratolimod (TLR7) provided no significant benefit to IgG levels and actively demonstrated an inhibitory effect on T-cell IFN-\gamma expression, with Telratolimod showing the most pronounced suppression of cellular immunity. Overall, these findings strongly support the continued development of saRNA as a viable vaccine modality for Marburg virus disease (MVD). Moving forward, additional studies are crucial to thoroughly elucidate the cellular interactions of these formulations and determine how the encapsulated TLR agonists interact with their respective receptors. Future research must also focus on evaluating the vaccine's potential to induce neutralizing antibody responses and establishing protective efficacy against viral challenges in relevant animal models, ultimately paving the way for optimized, deployment-ready countermeasures against potential Marburg outbreaks.

Conflicts of interest

There are no conflicts to declare.

Data availability

Data are available from the corresponding author upon reasonable request.

Animal Care and Use Statement

All animal procedures were performed in accordance with the Guidelines for Care and Use of Laboratory Animals of the U.S. Department of Agriculture's (USDA) Animal Welfare Act (9 CFR Parts 1, 2, and 3); the Guide for the Care and Use of Laboratory Animals (Institute of Laboratory Animal Resources, National Academy Press, Washington, D.C., 2011); and the National Institutes of Health, Office of Laboratory Animal Welfare (OLAW). All procedures were reviewed and approved by Labcorp, Early Development Laboratories Institutional Animal Care and Use Committee (IACUC) and Institutional Biosafety Committee (IBC). The Labcorp facility is

View Article Online
DOI: 10.1039/D6PM00134C

accredited by the Associated for Assessment and Accreditation of Laboratory Animal Care (AAALAC).

Acknowledgement

The authors would like to thank Lee Metcalf and his team at Centre for Process Innovation (CPI), Darlington UK. The authors also would like to thank Professor Jamie Blaza at the department of chemistry, University of York for his support in Electron cryo-microscopy.

View Article Online
DOI: 10.1039/D6PM00134C

References

1. *WHO Pathogens Prioritization*. (2024).

2. Abir, M. H. *et al.* Pathogenicity and virulence of Marburg virus. *Virulence* **13**, 609–633 (2022).

3. Srivastava, S. *et al.* Emergence of Marburg virus: a global perspective on fatal outbreaks and clinical challenges. *Front. Microbiol.* **14**, (2023).

4. Cross, R. W. *et al.* An introduction to the Marburg virus vaccine consortium, MARVAC. *PLoS Pathog.* **18**, 1–10 (2022).

5. Suschak, J. J. & Schmaljohn, C. S. Vaccines against Ebola virus and Marburg virus: recent advances and promising candidates. *Hum. Vaccines Immunother.* **15**, 2359–2377 (2019).

6. Hashiguchi, T. *et al.* Structural Basis for Marburg Virus Neutralization by a Cross-Reactive Human Antibody. *Cell* **160**, 904–912 (2015).

7. Hamer, M. J. *et al.* Safety, tolerability, and immunogenicity of the chimpanzee adenovirus type 3-vectored Marburg virus (cAd3-Marburg) vaccine in healthy adults in the USA: a first-in-human, phase 1, open-label, dose-escalation trial. *Lancet* **401**, 294–302 (2023).

8. Andrea, M. *et al.* DC-SIGN and DC-SIGNR Interact with the Glycoprotein of Marburg Virus and the S Protein of Severe Acute Respiratory Syndrome Coronavirus. *J. Virol.* **78**, 12090–12095 (2004).

9. Andrea, M. *et al.* DC-SIGN and DC-SIGNR Interact with the Glycoprotein of Marburg Virus and the S Protein of Severe Acute Respiratory Syndrome Coronavirus. *J. Virol.* **78**, 12090–12095 (2004).

10. Comes, J. D. G., Pijlman, G. P. & Hick, T. A. H. Rise of the RNA machines – self-amplification in mRNA vaccine design. *Trends Biotechnol.* **41**, 1417–1429 (2023).

11. Casmil, I. C. *et al.* The advent of clinical self-amplifying RNA vaccines. *Mol. Ther.* **33**, 2565–2582 (2025).

12. Bloom, K., van den Berg, F. & Arbuthnot, P. Self-amplifying RNA vaccines for infectious diseases. *Gene Ther.* **28**, 117–129 (2021).

13. Tomeh, M. A. *et al.* Stiffness-tuneable nanocarriers for controlled delivery of ASC-J9 into colorectal cancer cells. *J. Colloid Interface Sci.* **594**, 513–521 (2021).

14. Tomeh, M. A., Hadianamrei, R., Xu, D., Brown, S. & Zhao, X. Peptide-functionalised magnetic silk nanoparticles produced by a swirl mixer for enhanced anticancer activity of ASC-J9. *Colloids Surfaces B Biointerfaces* **216**, 112549 (2022).

15. Hou, X., Zaks, T., Langer, R. & Dong, Y. Lipid nanoparticles for mRNA delivery. *Nat. Rev. Mater.* **6**, 1078–1094 (2021).

16. Sandbrink, J. B. & Shattock, R. J. RNA Vaccines: A Suitable Platform for Tackling Emerging Pandemics? *Front. Immunol.* **11**, 1–9 (2020).

17. Tomeh, M. A. Design and development of novel nanocarriers for targeted drug delivery. at (2021).

View Article Online
DOI: 10.1039/D6PM00134C

18. Tomeh, M. A., Mansor, M. H., Hadianamrei, R., Sun, W. & Zhao, X. Optimization of large-scale manufacturing of biopolymeric and lipid nanoparticles using microfluidic swirl mixers. *Int. J. Pharm.* **620**, 121762 (2022).

19. Meyer, M. *et al.* Modified mRNA-Based Vaccines Elicit Robust Immune Responses and Protect Guinea Pigs from Ebola Virus Disease. *J. Infect. Dis.* **217**, 451–455 (2018).

20. Krähling, V. *et al.* Self-amplifying RNA vaccine protects mice against lethal Ebola virus infection. *Mol. Ther.* **31**, 374–386 (2023).

21. Bukreyev, A. *et al.* Divergent antibody recognition profiles are generated by protective mRNA vaccines against Marburg and Ravn viruses. *Res. Sq.* 1–30 (2024) doi:10.21203/rs.3.rs-4087897/v1.

22. Tomeh, M. A., Smith, R. K. & Watkinson, A. Recent Developments of RNA Vaccines and Therapeutics: Reagents, Formulations, and Characterization. *Mol. Pharm.* **22**, 5257–5282 (2025).

23. Walter, A. *et al.* Aldara activates TLR7-independent immune defence. *Nat. Commun.* **4**, 1–13 (2013).

24. Pulendran, B., S. Arunachalam, P. & O'Hagan, D. T. Emerging concepts in the science of vaccine adjuvants. *Nat. Rev. Drug Discov.* **20**, 454–475 (2021).

25. Brito, L. A. & O'Hagan, D. T. Designing and building the next generation of improved vaccine adjuvants. *J. Control. Release* **190**, 563–579 (2014).

26. Meric-Bernstam, F., Larkin, J., Tabernero, J. & Bonini, C. Enhancing anti-tumour efficacy with immunotherapy combinations. *Lancet* **397**, 1010–1022 (2021).

27. Fitzgerald, K. A. & Kagan, J. C. Toll-like Receptors and the Control of Immunity. *Cell* **180**, 1044–1066 (2020).

28. Choi, H. *et al.* Integration of TLR7/8 agonists into lipid nanoparticles enhances antigen-specific immune responses to N1-methyl-Ψ-modified mRNA-LNP vaccines. *J. Biol. Eng.* **19**, 103 (2025).

29. Dongye, Z., Li, J. & Wu, Y. Toll-like receptor 9 agonists and combination therapies: strategies to modulate the tumour immune microenvironment for systemic anti-tumour immunity. *Br. J. Cancer* **127**, 1584–1594 (2022).

30. O'Neill, L. A. J., Golenbock, D. & Bowie, A. G. The history of Toll-like receptors — redefining innate immunity. *Nat. Rev. Immunol.* **13**, 453–460 (2013).

31. Moghimi, S. M. & Simberg, D. Pro-inflammatory concerns with lipid nanoparticles. *Molecular therapy : the journal of the American Society of Gene Therapy* vol. 30 2109–2110 at https://doi.org/10.1016/j.ymthe.2022.04.011 (2022).

32. Tahtinen, S. *et al.* IL-1 and IL-1ra are key regulators of the inflammatory response to RNA vaccines. *Nat. Immunol.* **23**, 532–542 (2022).

33. Monie, A., Hung, C. F., Roden, R. & Wu, T. C. Cervarix™:A vaccine for the prevention of HPV 16, 18-associated cervical cancer. *Biol. Targets Ther.* **2**, 107–113 (2008).

34. Heineman, T. C., Cunningham, A. & Levin, M. Understanding the immunology of Shingrix, a recombinant glycoprotein E adjuvanted herpes zoster vaccine. *Curr. Opin. Immunol.* **59**, 42–48 (2019).

View Article Online
DOI: 10.1039/D6PM00134C

35. Lim, G.-H. L. & S.-G. CpG-Adjuvanted Hepatitis B Vaccine (HEPLISAV-B®) Update. *Expert Rev. Vaccines* **20**, 487–495 (2021).

36. Kitandwe, P. K. *et al.* A Lipid Nanoparticle-Formulated Self-Amplifying RNA Rift Valley Fever Vaccine Induces a Robust Humoral Immune Response in Mice. *Vaccines* **12**, (2024).

37. Brader, M. L. *et al.* Encapsulation state of messenger RNA inside lipid nanoparticles. *Biophys. J.* **120**, 2766–2770 (2021).

38. Simonsen, J. B. A perspective on bleb and empty LNP structures. *J. Control. Release* **373**, 952–961 (2024).

39. Cheng, M. H. Y. *et al.* Induction of Bleb Structures in Lipid Nanoparticle Formulations of mRNA Leads to Improved Transfection Potency. *Adv. Mater.* **35**, 2303370 (2023).

40. Kloczewiak, M., Banks, J. M., Jin, L. & Brader, M. L. A Biopharmaceutical Perspective on Higher-Order Structure and Thermal Stability of mRNA Vaccines. *Mol. Pharm.* **19**, 2022–2031 (2022).

41. Morefield, G. L., Hawkins, L. D., Ishizaka, S. T., Kissner, T. L. & Ulrich, R. G. Synthetic toll-like receptor 4 agonist enhances vaccine efficacy in an experimental model of toxic shock syndrome. *Clin. Vaccine Immunol.* **14**, 1499–1504 (2007).

42. Gopalakrishnan, A. *et al.* E6020, a TLR4 Agonist Adjuvant, Enhances Both Antibody Titers and Isotype Switching in Response to Immunization with Hapten-Protein Antigens and Is Diminished in Mice with TLR4 Signaling Insufficiency. *J. Immunol.* **209**, 1950–1959 (2022).

43. Kalina, W. V., Warfield, K. L., Olinger, G. G. & Bavari, S. Discovery of common marburgvirus protective epitopes in a BALB/c mouse model. *Virol. J.* **6**, (2009).

44. Rahim, M. N. *et al.* Complete protection of the BALB/c and C57BL/6J mice against Ebola and Marburg virus lethal challenges by pan-filovirus T-cell epigraph vaccine. *PLoS Pathog.* **15**, 1–17 (2019).

45. Locksley, R. M. *et al.* Induction of Th1 and Th2 CD4+ subsets during murine Leishmania major infection. *Res. Immunol.* **142**, 28–32 (1991).

46. Fornefett, J. *et al.* Comparative analysis of humoral immune responses and pathologies of BALB/c and C57BL/6 wildtype mice experimentally infected with a highly virulent Rodentibacter pneumotropicus (Pasteurella pneumotropica) strain. *BMC Microbiol.* **18**, 1–11 (2018).

47. Jovicic, N. *et al.* Differential immunometabolic phenotype in Th1 and Th2 dominant mouse strains in response to high-fat feeding. *PLoS One* **10**, 1–21 (2015).

48. Liang, F. *et al.* Efficient Targeting and Activation of Antigen-Presenting Cells In Vivo after Modified mRNA Vaccine Administration in Rhesus Macaques. *Mol. Ther.* **25**, 2635–2647 (2017).

49. Carter, D. *et al.* The success of toll-like receptor 4 based vaccine adjuvants. *Vaccine* **61**, 127413 (2025).

50. Zhao, T. *et al.* Vaccine adjuvants: mechanisms and platforms. *Signal Transduct. Target. Ther.* **8**, (2023).

View Article Online
DOI: 10.1039/D6PM00134C

51. Kang, D. D. *et al.* Targeting and tracking mRNA lipid nanoparticles at the particle, transcript and protein level. *Nat. Biomed. Eng.* **9**, 1591–1609 (2025).

52. Hamilton, A. G. *et al.* High-Throughput In Vivo Screening Identifies Differential Influences on mRNA Lipid Nanoparticle Immune Cell Delivery by Administration Route. *ACS Nano* **18**, 16151–16165 (2024).

53. Lu, Z. R. & Sun, D. Mechanism of pH-sensitive Amphiphilic Endosomal Escape of Ionizable Lipid Nanoparticles for Cytosolic Nucleic Acid Delivery. *Pharm. Res.* **42**, 1065–1077 (2025).

54. Wiest, M. J. *et al.* Disruption of endosomal trafficking with EGA alters TLR9 cytokine response in human plasmacytoid dendritic cells. *Front. Immunol.* **14**, 1–14 (2023).

55. Mishra, H. *et al.* Disrupted degradative sorting of TLR7 is associated with human lupus. *Sci. Immunol.* **9**, (2024).

56. Chaudhary, N. *et al.* Amine headgroups in ionizable lipids drive immune responses to lipid nanoparticles by binding to the receptors TLR4 and CD1d. *Nat. Biomed. Eng.* doi:10.1038/s41551-024-01256-w.

View Article Online
DOI: 10.1039/D6PM00134C

Data availability

Data are available from the corresponding author upon reasonable request.